Pure Shift NMR in Continuous Flow

Margherita Bazzoni, Armand Régheasse, Elsa Caytan, François-Xavier Felpin, Patrick Giraudeau, Aurélie Bernard, Ralph Adams, Gareth Morris, Mathias J Nilsson, Jean-Nicolas Dumez

Chemistry–A European Journal
Research Article
doi.org/10.1002/chem.202403385
Chemistry Europe
European Chemical Societies Publishing
www.chemeurj.org

Pure Shift NMR in Continuous Flow

Margherita Bazzoni,[a] Armand Régheasse,[a] Elsa Caytan,[b] François-Xavier Felpin,[a] Patrick Giraudeau,[a] Aurélie Bernard,[a] Ralph W. Adams,[c] Gareth A. Morris,[c] Mathias Nilsson,[c] and Jean-Nicolas Dumez*[a]

Flow NMR is an expanding analytical approach with applications that include in-line analysis for process control and optimisation, and real-time reaction monitoring. The samples monitored by flow NMR are typically mixtures that yield complex 1D ^{1}H spectra. "Pure shift" NMR is a powerful approach to simplifying ^{1}H NMR spectra, but its standard implementation is not compatible with continuous flow because of interference between sample motion and the position-dependent spin manipulations that are required in pure shift NMR. Here we show that pure shift NMR spectra can be successfully collected for continuously flowing samples, thanks to an adapted acquisition scheme, robust solvent suppression, and a velocity-compensation strategy. The resulting method is used to collect ultrahigh resolution reaction monitoring data. Pure shift NMR spectra are expected to benefit many applications of flow NMR.

Introduction

Nuclear magnetic resonance (NMR) spectroscopy is a powerful analytical tool, which provides extensive structural and quantitative information on samples ranging from complex mixtures of small molecules to macromolecules and supramolecular assemblies. It is increasingly being applied to flowing samples, for example in flow chemistry, high throughput NMR, and reaction monitoring.[1–4] Notably, online monitoring by flow NMR makes it possible to achieve real-time monitoring over a broad range of experimental conditions that would be difficult or impossible to replicate within a spectrometer.[5,6] In this approach, the reaction is carried out in a reactor outside the magnet, and a fraction of the reaction mixture is continuously circulated through the NMR probe for analysis and then back to the reactor.[2,7–10] Applications have also been reported that range from biological systems to batteries.[11–13] Flow NMR is also powerful for efficiently analysing the outcome of a reaction or process, with a strong potential for automation and active feedback.[14] It has for example been used to analyse directly the output of a flow reactor, for both small molecules and polymers.[15,16] Flow methods are also key to hyphenating NMR spectroscopy with chromatographic separation.[1] Flow NMR has become particularly widespread with the advent of benchtop NMR spectrometers, although these have limited sensitivity and resolution. The design of custom and commercial flow cells that are compatible with standard high-field instrumentation has expanded the application of flow NMR, allowing the analysis of a broad range of chemical reactions.[9,10,12,15,17,18]

Standard NMR monitoring approaches typically rely on 1D ^{1}H spectra, which are fast to acquire and provide good sensitivity.[19–21] However, these spectra are often complex, due to signal overlap, which can prevent compound identification and the accurate measurement of integrals. A number of methods are available to address the complexity of mixture spectra in static conditions (i.e., in the absence of flow). These include 2D NMR methods[22–24] that provide extra signal dispersion along an additional dimension, diffusion-based methods[25–27] that help identify signals that originate from the same compound, and homonuclear decoupling methods that effectively suppress the effect of J couplings and thus collapse ^{1}H multiplets into singlets, resulting in "pure shift" spectra.[28–30] The possibility to use such methods for a continuously flowing sample is key to addressing applications in, e.g., reaction and process monitoring.

Sample flow poses significant problems for many NMR experiments, especially those that rely on magnetic field gradient pulses. While these methods operate well for the stationary samples for which they were designed, any net movement between gradient pulses can cause a phase shift in the signal, commonly resulting in a loss of signal intensity. As a result, original flow-compatible methods have been developed over recent years. For example, ultrafast 2D NMR based on spatial parallelisation requires the use of field gradient pulses along a transverse axis to avoid sensitivity losses due to sample motion.[17] For diffusion NMR, the combined use of a transverse encoding axis and velocity-compensation schemes was found to yield accurate results for samples monitored by flow NMR.[31] For homonuclear decoupling methods, it was recently shown

[a] M. Bazzoni, A. Régheasse, F.-X. Felpin, P. Giraudeau, A. Bernard, J.-N. Dumez
Nantes Université, CNRS, CEISAM UMR6230, Nantes, France
E-mail: jean-nicolas.dumez@univ-nantes.fr
[b] E. Caytan
ISCR – UMR6226, Univ. Rennes, CNRS, Rennes, France
[c] R. W. Adams, G. A. Morris, M. Nilsson
Department of Chemistry, University of Manchester, Manchester, UK

Supporting information for this article is available on the WWW under https://doi.org/10.1002/chem.202403385

that velocity compensation can be achieved by appropriate setup of available NMR pulse sequences, and this enabled the acquisition of pure shift spectra with full sensitivity even in the presence of strong convection.[32] Such pure shift spectra have never been demonstrated, however, with a flow NMR setup, which introduces additional complications such as flow pulsation, in/out-flow effects, and the requirement to work with non-deuterated solvents.

In this work, we show that high-quality pure shift NMR spectra can be acquired for a continuously flowing sample, thanks to the use of a solvent-suppression scheme, velocity-compensating gradient waveforms, and an adapted data sampling strategy. We illustrate the utility of this approach with the online monitoring of a tosylation reaction. The gain in resolution with pure shift NMR makes it possible to resolve peaks that are overlapped in conventional 1D ^{1}H spectra. The comparison of decoupled and conventional spectra shows that the former can also be used to track the relative concentrations of compounds during a chemical reaction. Overall, flow-compatible pure shift NMR should broaden the range of applications that can be addressed by flow NMR.

Results and Discussion

The "Zangger-Sterk" (ZS) NMR method[33] is a well-established way to achieve broadband homonuclear decoupling and obtain pure shift NMR spectra. A convection-compensated version was recently described,[32] which has potential for use with flow. Figure 1 shows the comparison between a conventional 1D ^{1}H (panel b) and a ZS 1D ^{1}H (panel c) spectrum for a sample of quinine in chloroform at a concentration of 250 mM, in the absence of flow. Homonuclear decoupling makes it possible to resolve signals that overlap in the conventional spectrum, e.g., in the 1.6–1.8 ppm, 2.9–3.1 ppm and 4.8–5.0 ppm regions. The pure shift spectrum was obtained using typical values for the pulse sequence parameters, in particular for the amplitudes of the coherence transfer pathway selection gradients. When the same experiment is carried out on a sample flowing at a rate of 1.5 mL/min, which is within the range typically employed for online monitoring by flow NMR, very significant sensitivity losses are observed, of greater than 90%, as shown in panel d.

In contrast, when the amplitudes of the gradient pulses employed during the sequence are adjusted to compensate for flow effects, most of the signal amplitude obtained on a non-flowing sample is recovered, as shown in panel e. This shows that velocity compensation for the ZS pulse sequence, which

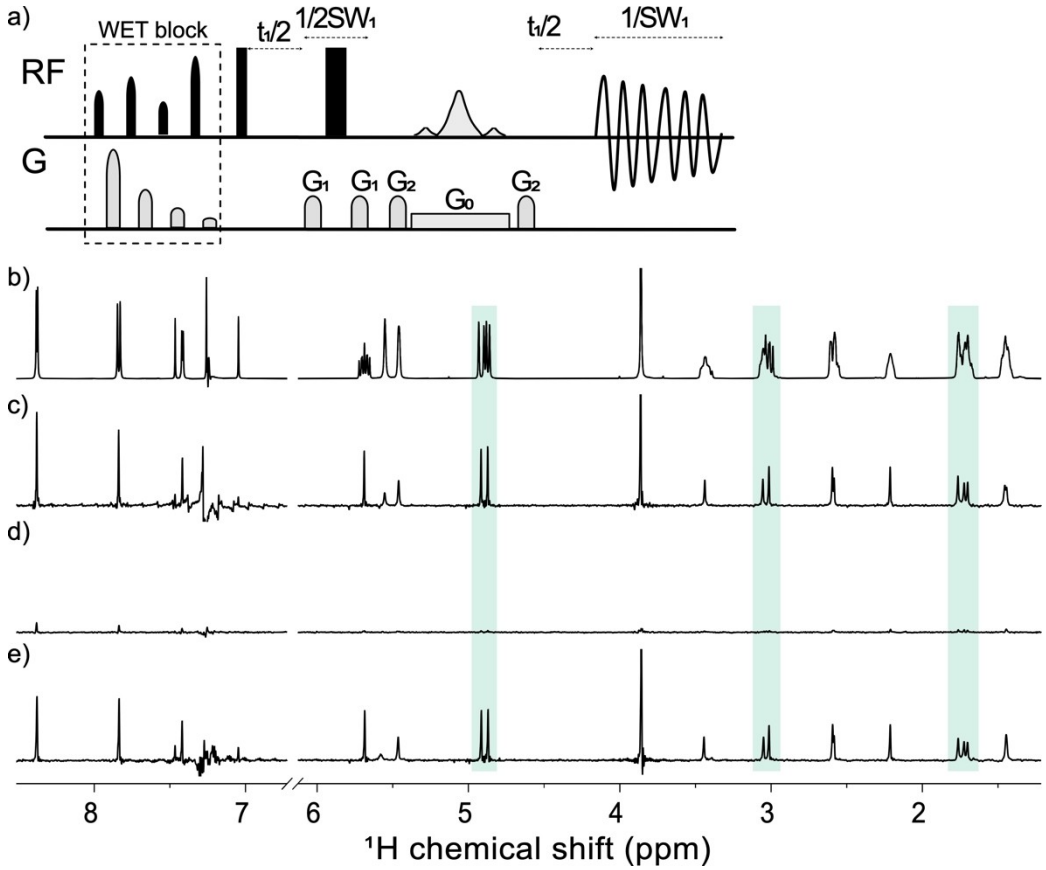

Figure 1. a) Zangger-Sterk pulse sequence with a WET block for solvent suppression; b) ^{1}H 1D spectrum of a quinine sample in chloroform; c) pure shift spectrum acquired for a static quinine sample with $G_2 = 0.05$ G/cm; d) pure shift spectrum acquired for a flowing (1.5 mL/min) quinine sample with $G_2 = 0.05$ G/cm; and e) pure shift spectrum acquired under the same conditions as d) but using flow-compensating gradients ($G_2 = -0.24$ G/cm). Highlighting shows regions that are affected by overlap in the conventional ^{1}H spectrum but well resolved in the pure shift spectra. The pure shift spectra shown in c) to e were obtained using interleaved sampling (see main text and Figure 2).

was initially demonstrated in the case of convection, is also effective in the case of net sample flow. These results additionally required the use of efficient solvent suppression, and of an original "interleaved" acquisition strategy. These three aspects are described in the following sections.

Flow Compensation

The results shown in Figure 1 were obtained on a spectrometer operating at a ^{1}H Larmor frequency of 500.13 MHz, using an inverse-detection probe equipped with triple-axis field gradients (Bruker Avance III and BBI). Flow NMR was implemented using a commercial flow tube (InsightMR, Bruker), which consists of a thermostatic transfer line containing two capillaries going to and from a 5 mm tube tip. The HPLC pump (Jasco) used delivers sufficiently consistent flow rates to obtain repeatable results. The pure shift spectra were measured using the pulse sequence shown in Figure 1a. The central element is the simultaneous application of a frequency-selective refocusing pulse with a narrow bandwidth (25 Hz here) and of a weak magnetic field gradient ($G_0 = 0.0063$ G/cm here). With this ZS element, each resonance in the spectrum is affected by the selective pulse only in a thin slice (0.09 mm) of the sample, the *z* position of which is a linear function of the chemical shift. Effectively, the spectrum is mapped onto the detection region of the sample tube. Within each slice, the ZS element acts to: (i) select the signals of spins that are refocused, the active spins, and suppress those of the others, the passive spins; and (ii) refocus the effect of J couplings between active and passive spins over the t_1 period. A chunk of data of duration $\tau \ll 1/J$ is then acquired for each value of t_1, where the choice of τ requires a compromise between the total duration of the experiment, and the purity of the decoupled spectrum. An indirect benefit of the ZS scheme is an increased robustness against field inhomogeneity, because each signal originates from just a thin slice of the sample.[34]

Applying a long, albeit weak, gradient G_0 during the ZS element, to nuclear spins that are moving at constant velocity in the same direction, results in an additional dephasing that is proportional to the velocity and to the area of the gradient pulse. While this could be tolerated if all the spins were moving at the same velocity, in the case of a velocity distribution it results in phase dispersion and thus undesirable signal attenuation. For the flow cell used here, the flow is typically laminar, resulting in the large signal losses shown in Figure 1d. There exist systematic approaches to selecting gradient waveforms to cancel flow effects, that are widely used in both spectroscopy and magnetic resonance imaging,[35,36] for example for convection compensation in diffusion measurements. In this case, velocity compensation of the slice-selective refocusing pulse can be obtained by the use of two gradient pulses (G_2), each of area $-A/2$, around the slice-selection gradient G_0 of area A, yielding the spectrum of Figure 1e. The dependence of the signal amplitude on velocity and gradient area has the expected sinc-like shape (see supporting information). Importantly, the gradient amplitude that gives velocity compensation ($G_2 = -G_0\delta_0/\delta_2$, where δ_i is the duration of the *i*th gradient) is independent of the actual velocity. In fact, a comparison of spectra acquired at different flow rates (see Figure S2 and S3), shows that the velocity compensation scheme is effective for flow rates of up to 4 mL/min.

The use of a pump that, as here, delivers minimal pulsation is probably key to obtaining sufficiently reproducible results, as the gradient waveform employed here compensates only for constant velocity flow and not for acceleration effects. The fact that the flow is laminar is also key to the success of the approach, as velocity compensation would fail for turbulent flow. For this flow cell geometry, the flow is found to be laminar for a broad range of solvent viscosity. In addition, it is interesting to note that spins that are in a given slice during the slice selection subsequently move at different velocities, depending on their distance from the tube axis, during the second half of the t_1 evolution delay. However, since no further position-dependent element is used in the sequence, this has no consequence for the results. It could, however, complicate the implementation of real-time ZS decoupling, which was not attempted here.

Working with a Fully Protonated Solvent

The acquisition of a high-quality spectrum such as that shown in Figure 1e also required facing the additional challenge of working with non-deuterated solvent, in which flow NMR experiments are typically carried out both for cost reasons and to avoid modifying reaction kinetics. However, the presence of a large unsuppressed solvent signal is highly detrimental, because of signal overlap and dynamic range problems. In this work, the WET[37] pulse sequence was found to efficiently suppress the chloroform signal at 7.26 ppm.

A side-effect of working without a deuterated solvent is that the time stability of the magnetic field (and of its spatial inhomogeneity) is reduced, due to the lack of a lock signal. This can be highly detrimental for pure shift (and 2D) experiments. Pure shift NMR spectra are obtained through Fourier transform of a time-domain signal that is reconstructed from multiple separate measurements.[28,33,38] Any systematic errors in this chunk-wise acquisition cause artefactual sidebands ("chunking artefacts") that originate from discontinuities in the envelope of the reconstructed signal, and effectively reduce the dynamic range of the signals detectable. The spectrum shown in Figure 2a, notably the methoxy signal at 3.8 ppm, shows that chunking artefacts can be problematic for spectra acquired on an unlocked sample (this is shown here for a flowing sample, but is also observed for an unlocked non-flowing sample). This is attributable to slow, uncompensated variations of the magnetic field. In standard pure shift experiments, all of the scans for a given t_1 increment are acquired before moving on to the next t_1 increment. If, however, an "interleaved" sampling strategy is used, chunking artefacts are greatly reduced, as shown in Figure 2b. The latter spectrum was obtained by looping on the t_1 incrementation first, and on the scan number second, so to minimise the variability between the different

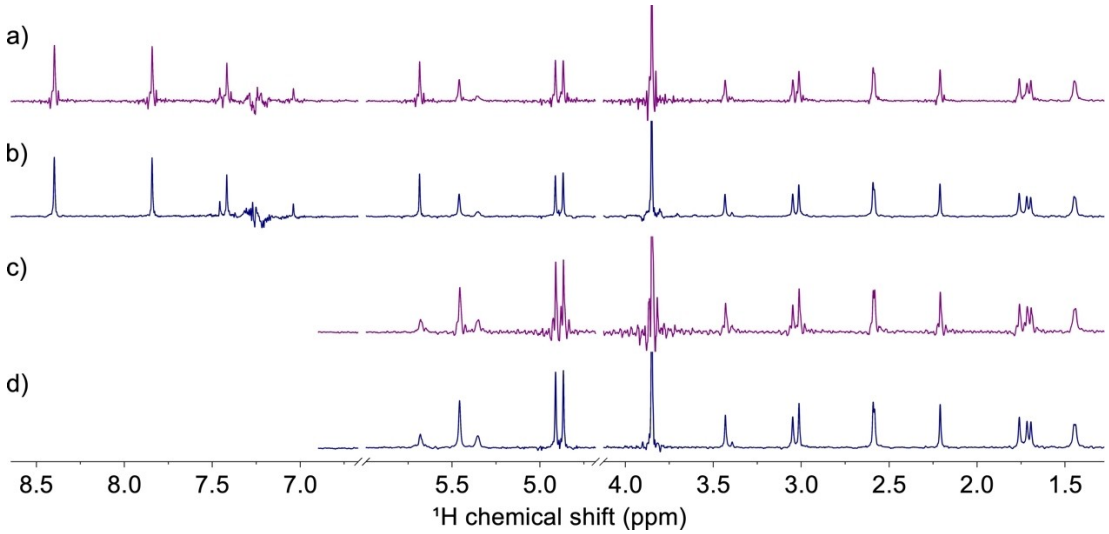

Figure 2. Zangger-Sterk spectra acquired on a quinine sample in $CHCl_3$ flowing at 1.5 mL/min using conventional (purple) vs. interleaved (blue) acquisition, for two different combinations of G_0, G_2, and O1P (frequency offset of the spectrum midpoint). a) and b) $G_0 = 0.0063$ G/cm, $G_2 = -0.24$ G/cm, O1P = 4.3 ppm, c) and d) $G_0 = 0.0047$ G/cm, $G_2 = -0.17$ G/cm, O1P = 1.9 ppm.

increments. As a result, all of the chunks represent averages over the effects of the different magnetic fields experienced during the whole acquisition. The interleaved acquisition scheme yields a cleaner baseline that is particularly important for regions of the spectra containing intense peaks, such as at 3.8 or 4.9 ppm. In the case of flow experiments, it is in principle possible for out-flow effects on the apparent transverse relaxation rate to exacerbate chunking artefacts, but no significant effects were observed in this work.

This interleaved sampling strategy is also beneficial for the analysis of samples that evolve in time. As in the case of field instability, the effect of systematic changes (in this case caused by changes in concentrations of the compounds) on the pure shift spectra is greatly reduced,

In ZS pure shift NMR, in cases where the solvent signal is well outside the region of the spectrum that is of interest, it can be advantageous to adjust the parameters of the ZS element (specifically the encoding gradient amplitude G_0 and the carrier frequency O1P) so that the solvent is not included in the acquired spectral window and thus among the active spins. As well as reducing interference from solvent signals, the concomitant decrease in the gradient G_0 gives an increase in signal-to-noise ratio (SNR). In combination with the WET element this yields further improvement in solvent signal suppression, as illustrated in Figures 2c and d. This approach was used for the reaction monitoring data discussed below. The interleaved sampling scheme was still found to bring improved signal-to-artefact ratio.

Reaction Monitoring

The solvent-suppressed and velocity-compensated pure shift NMR pulse sequence shown in Figure 1a was tested on the monitoring of the tosylation of menthol (Figure 3) in chloroform. Preliminary studies to evaluate the appropriateness of the reaction and its timescale were conducted in a standard NMR tube. A reaction solution was prepared by mixing 39.0 mg of menthol, 53.9 mg of tosyl chloride (TsCl) and 54.0 mg of 4-dimethylaminopyridine (DMAP) in 1.0 mL of $CHCl_3$. 0.5 mL of this solution was transferred to an NMR tube to allow the reaction evolution to be followed inside the spectrometer. The pure shift spectra acquired during the reaction are shown in Figure S4. Interestingly, the utility of the interleaved acquisition scheme for unlocked NMR reaction monitoring is clearly visible in this case also, with a signal-to-artefact ratio that is much higher with interleaved sampling.

These results allowed the successful setting up of flow monitoring of the same reaction. A solution of 1.28 g of TsCl and 0.99 g of menthol in 24 mL of $CHCl_3$ was prepared and was pumped through the spectrometer flow cell at a flow rate of 1.2 mL/min. Before closing the recycling loop, 5.25 mL of solution was discarded in order to minimise dilution by residual solvent present in the system. The flow rate was stabilised at 1.2 mL/min, and reference WET-^{1}H and WET-pure shift spectra were acquired. While the mixture was continuously recirculating between reactor and NMR probe, the reaction was initiated by adding progressively a DMAP solution (1.06 g of DMAP in 2 mL of $CHCl_3$). 65% of that solution was initially added drop-wise (starting at time 0 of the *x*-axis in Figure 3). After 32 min, based on the observed reaction progress, the remaining 35% was added. For the monitoring, WET-pure shift spectra were acquired alternately with WET-^{1}H spectra. The pure shift spectra were focused on the aliphatic region of the sample, using a smaller encoding gradient and thus increasing the SNR. Each pure shift spectrum was obtained using 4 scans, with a 4-step phase cycle, and 16 t_1 increments, resulting in a duration of 5 min per spectrum. This duration is often suitable for online monitoring by flow NMR. For much faster reactions, real-time or semi-real time experiments could in principle be used[39–41], but

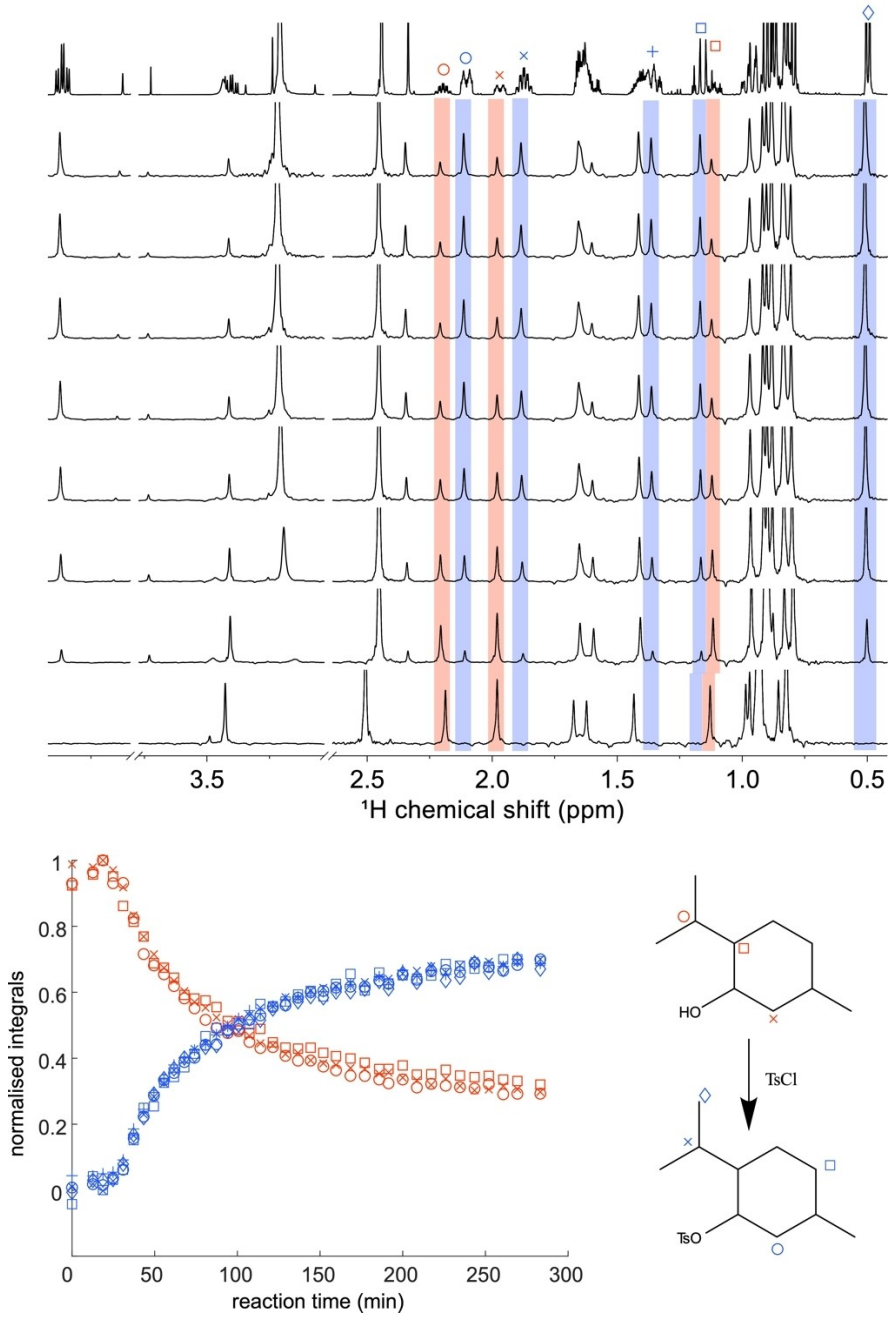

Figure 3. ZS pure shift spectra acquired during monitoring of a flowing reaction mixture (1.2 mL/min), and integrals of selected peaks as function of reaction time. All data were normalised to the sums of the integrals of reactants and products, assumed to be unchanged throughout reaction (i.e. it was assumed that no side-reactions were present), in order to compensate for the initial dilution caused by the DMAP addition. Reagent integrals (red) were then normalised to 1 at the start of the reaction, and product integrals (blue) were normalised to a final value of 0.7, since at the end of the monitoring 30 % of the menthol was still present. This again assumes that the reaction does not generate any by-products, as confirmed by the absence of extraneous signals in the experimental spectra.

flow compensated versions of these are still under development.

Reaction monitoring data obtained with the solvent-suppressed and velocity-compensated pulse sequence using interleaved sampling are shown in Figure 3. High-quality pure shift spectra were obtained throughout the reaction. The integrals of a selection of peaks as a function of time are shown in Figure 3. Homonuclear decoupling here makes it possible to resolve and integrate peaks that overlap in the conventional 1D ^{1}H spectrum, for example in the 1.10–1.19 and 1.34–1.44 ppm regions, and to track the relative concentrations of the corresponding compounds. Absolute concentration would require a calibration step, because of the peak-specific response found in pure shift spectra (due to the effects of frequency offsets, J couplings, and translational diffusion), or the use of a variable number of iterations of the pulse sequence element in

order to determine the site-specific attenuation and hence to extrapolate back to the loss-free signal.[42] In this case, some peaks are also resolvable in the conventional, non-decoupled, 1D ^{1}H spectrum, and they were used to provide data, shown in Figure S5, that validate the concentration time courses obtained from the pure shift spectra.

In pure shift NMR, increased resolution comes at a price in sensitivity. With Zangger-Sterk decoupling, a compromise is required between decoupling quality and signal intensity, and between spectral width and signal intensity. The signal intensities seen in pure shift spectra are typically 1 to 20%, sometimes even less, of those in the corresponding non-decoupled spectrum, depending on the decoupling method used. Here, on the quinine sample at a concentration of 250 mM, an SNR of about 100 is obtained for CH signals, which would translate into limits of detection in the low millimolar range. The utility of pure shift NMR is application-dependent, but it is expected to be very suitable for organic chemical reactions with starting concentrations above 100 mM.

Other pure shift methods offer different compromises between spectrum quality and sensitivity, and they are also expected to be differently sensitive to flow effects. While BIRD decoupling can be implemented without long gradient pulses, it is not as general as ZS decoupling. PSYCHE decoupling, on the other hand, was found to be applicable in the presence of strong convection, and will be the topic of future investigations on continuously flowing samples.

Conclusions

We have shown that high-quality pure shift ^{1}H NMR spectra can be obtained for a continuously flowing sample, thanks to the use of a velocity-compensated gradient waveform, efficient solvent suppression, and interleaved data sampling. The approach was illustrated with the monitoring of a tosylation reaction, for which overlapping multiplets become well resolved singlets thanks to the use of pure shift NMR. The resulting signal integrals can be used for relative quantification of the compounds as a function or reaction time. Pure shift flow NMR can thus provide access to kinetic and structural information that is otherwise buried in overlapping multiplets. It should prove useful for the many applications of flow NMR, including online and in-line reaction and process monitoring.

Acknowledgements

The authors thank Carine van Heijenoort and Ewen Lescop for the help to implement interleaved sampling. This work has received funding from the European Research Council (ERC) under the European Union's Horizon 2020 research and innovation program (grant agreement no 801774/DINAMIX and 814747/SUMMIT) the Region Pays de la Loire (Connect Talent HP NMR), and a Royal Society International Exchange Scheme (IES\R1\221028). The authors also acknowledge the French National Infrastructure for Metabolomics and Fluxomics MetaboHUB-ANR-11-INBS-0010 (www.metabohub.fr) and the Corsaire metabolomics core facility (Biogenouest). This work includes NMR experiments carried out on the CEISAM NMR platform.

Conflict of Interests

The authors declare no conflict of interest.

Data Availability Statement

The data was uploaded on Zenodo, at this link: https://doi.org/10.5281/zenodo.12806894.

Keywords: Flow NMR · Reaction monitoring · Pure shift NMR

[1] P. A. Keifer, in *Annu. Rep. NMR Spectrosc*, (Ed.: G. A. Webb), Academic Press, **2007**, 1–47.
[2] A. Martínez-Carrión, M. G. Howlett, C. Alamillo-Ferrer, A. D. Clayton, R. A. Bourne, A. Codina, A. Vidal-Ferran, R. W. Adams, J. Burés, *Angew. Chem. Int. Ed.* **2019**, *58*, 10189–10193.
[3] M. V. Gomez, A. de la Hoz, *Beilstein J. Org. Chem.* **2017**, *13*, 285–300.
[4] A. M. R. Hall, J. C. Chouler, A. Codina, P. T. Gierth, J. P. Lowe, U. Hintermair, *Catal. Sci. Technol.* **2016**, *6*, 8406–8417.
[5] D. A. Foley, E. Bez, A. Codina, K. L. Colson, M. Fey, R. Krull, D. Piroli, M. T. Zell, B. L. Marquez, *Anal. Chem.* **2014**, *86*, 12008–12013.
[6] A. M. R. Hall, P. Dong, A. Codina, J. P. Lowe, U. Hintermair, *ACS Catal.* **2019**, *9*, 2079–2090.
[7] D. A. Foley, A. L. Dunn, M. T. Zell, *Magn. Reson. Chem.* **2016**, *54*, 451–456.
[8] M. Khajeh, M. A. Bernstein, G. A. Morris, *Magn. Reson. Chem.* **2010**, *48*, 516–522.
[9] A. M. R. Hall, R. Broomfield-Tagg, M. Camilleri, D. R. Carbery, A. Codina, D. T. E. Whittaker, S. Coombes, J. P. Lowe, U. Hintermair, *Chem. Commun.* **2017**, *54*, 30–33.
[10] M. V. Silva Elipe, A. Cherney, R. Krull, N. Donovan, J. Tedrow, D. Pooke, K. L. Colson, *Org. Process Res. Dev.* **2020**, *24*, 1428–1434.
[11] M. Tabatabaei Anaraki, R. Dutta Majumdar, N. Wagner, R. Soong, V. Kovacevic, E. J. Reiner, S. P. Bhavsar, X. Ortiz Almirall, D. Lane, M. J. Simpson, H. Heumann, S. Schmidt, A. J. Simpson, *Anal. Chem.* **2018**, *90*, 7912–7921.
[12] L. Cerofolini, S. Giuntini, L. Barbieri, M. Pennestri, A. Codina, M. Fragai, L. Banci, E. Luchinat, E. Ravera, *Biophys. J.* **2019**, *116*, 239–247.
[13] E. W. Zhao, T. Liu, E. Jónsson, J. Lee, I. Temprano, R. B. Jethwa, A. Wang, H. Smith, J. Carretero-González, Q. Song, C. P. Grey, *Nature* **2020**, *579*, 224–228.
[14] P. Giraudeau, F.-X. Felpin, *React. Chem. Eng.* **2018**, *3*, 399–413.
[15] M. Bazzoni, C. Lhoste, J. Bonnet, K. E. Konan, A. Bernard, P. Giraudeau, F.-X. Felpin, J.-N. Dumez, *Chem. – Eur. J.* **2023**, *29*, e202203240.
[16] J. H. Vrijsen, I. A. Thomlinson, M. E. Levere, C. L. Lyall, M. G. Davidson, U. Hintermair, T. Junkers, *Polym. Chem.* **2020**, *11*, 3546–3550.
[17] C. Lhoste, M. Bazzoni, J. Bonnet, A. Bernard, F.-X. Felpin, P. Giraudeau, J.-N. Dumez, *Analyst* **2023**, *148*, 5255–5261.
[18] A. Sarkar, G. Dong, J. Quaglia-Motta, K. Sackett, *J. Pharm. Sci.* **2024**, *113*, 900–905.
[19] D. A. Foley, J. Wang, B. Maranzano, M. T. Zell, B. L. Marquez, Y. Xiang, G. L. Reid, *Anal. Chem.* **2013**, *85*, 8928–8932.
[20] M. Maiwald, H. H. Fischer, Y.-K. Kim, K. Albert, H. Hasse, *J. Magn. Reson.* **2004**, *166*, 135–146.
[21] O. Steinhof, G. Scherr, H. Hasse, *Magn. Reson. Chem.* **2016**, *54*, 457–476.
[22] M. Elyashberg, *TrAC Trends Anal. Chem.* **2015**, *69*, 88–97.
[23] M. Gal, M. Mishkovsky, L. Frydman, *J. Am. Chem. Soc.* **2006**, *128*, 951–956.
[24] M. J. Jaroszewicz, M. Liu, J. Kim, G. Zhang, Y. Kim, C. Hilty, L. Frydman, *Nat. Commun.* **2022**, *13*, 833.
[25] M. Khajeh, A. Botana, M. A. Bernstein, M. Nilsson, G. A. Morris, *Anal. Chem.* **2010**, *82*, 2102–2108.
[26] M. Oikonomou, J. Asencio-Hernández, A. H. Velders, M.-A. Delsuc, *J. Magn. Reson.* **2015**, *258*, 12–16.

[27] O. Tooley, W. Pointer, R. Radmall, M. Hall, T. Swift, J. Town, C. Aydogan, T. Junkers, P. Wilson, D. Lester, D. Haddleton, *ACS Polym. Au* **2024**, DOI: 10.1021/acspolymersau.4c00020.
[28] K. Zangger, *Prog. Nucl. Magn. Reson. Spectrosc.* **2015**, *86–87*, 1–20.
[29] M. Foroozandeh, G. A. Morris, M. Nilsson, *Chem. – Eur. J.* **2018**, *24*, 13988–14000.
[30] J. A. Aguilar, S. Faulkner, M. Nilsson, G. A. Morris, *Angew. Chem. Int. Ed.* **2010**, *49*, 3901–3903.
[31] A. Marchand, R. Mishra, A. Bernard, J. Dumez, *Chem. – Eur. J.* **2022**, *28*, e202201175.
[32] E. Caytan, H. M. Foster, L. Castañar, R. W. Adams, M. Nilsson, G. A. Morris, *Chem. Commun.* **2023**, *59*, 12633–12636.
[33] K. Zangger, H. Sterk, *J. Magn. Reson.* **1997**, *124*, 486–489.
[34] G. E. Wagner, P. Sakhaii, W. Bermel, K. Zangger, *Chem. Commun.* **2013**, *49*, 3155–3157.
[35] A. Jerschow, N. Müller, *J. Magn. Reson.* **1998**, *132*, 13–18.
[36] P. T. Callaghan, *Principles of Nuclear Magnetic Resonance Microscopy*, Oxford University Press, Oxford, New York, **1993**.
[37] R. J. Ogg, R. B. Kingsley, J. S. Taylor, *J. Magn. Reson. B* **1994**, *104*, 1–10.
[38] L. Castañar, T. Parella, *Magn. Reson. Chem.* **2015**, *53*, 399–426.
[39] A. Lupulescu, G. L. Olsen, L. Frydman, *J. Magn. Reson. San Diego Calif 1997* **2012**, *218*, 141–146.
[40] N. H. Meyer, K. Zangger, *Angew. Chem. Int. Ed.* **2013**, *52*, 7143–7146.
[41] P. Kiraly, M. Nilsson, G. A. Morris, *J. Magn. Reson.* **2018**, *293*, 19–27.
[42] H. M. Foster, M. Nilsson, R. W. Adams, G. A. Morris, *Anal. Chem.* **2024**, *96*, 9601–9609.

Manuscript received: October 17, 2024
Accepted manuscript online: October 21, 2024
Version of record online: November 13, 2024